RISØ

Risø-R-1543(EN)

Aerodynamic investigation of Winglets on Wind Turbine Blades using CFD

Jeppe Johansen and Niels N. Sørensen

Risø National Laboratory
Roskilde
Denmark
February 2006

Author: Jeppe Johansen and Niels N. Sørensen
Title: Aerodynamic investigation of Winglets on Wind Turbine Blades using CFD
Department: Wind Energy Department

Risø-R-1543(EN)
February 2006

Abstract (max. 2000 char.):

The present report describes the numerical investigation of the aerodynamics around a wind turbine blade with a winglet using Computational Fluid Dynamics, CFD.

Five winglets were investigated with different twist distribution and camber. Four of them were pointing towards the pressure side (upstream) and one was pointing towards the suction side (downstream). Additionally, a rectangular modification of the original blade tip was designed with the same planform area as the blades with winglets.

Results show that adding a winglet to the existing blade increase the force distribution on the outer approx 14 % of the blade leading to increased produced power of around 0.6% to 1.4% for wind speeds larger than 6 m/s. This has to be compared to the increase in thrust of around 1.0% to 1.6%. Pointing the winglet downstream increases the power production even further.

The effect of sweep and cant angles is not accounted for in the present investigation and could improve the winglets even more.

ISSN 0106-2840
ISBN 87-550-3497-7

Contract no.:
ENS-33031-0077

Group's own reg. no.:
1110047-01

Sponsorship:

Cover :

Pages: 17
Tables:2
References:5

Risø National Laboratory
Information Service Department
P.O.Box 49
DK-4000 Roskilde
Denmark
Telephone +45 46774004
bibl@risoe.dk
Fax +45 46774013
www.risoe.dk

Contents

Introduction

The following report is made during the EFP 2005 project “Program for Forskning i Anvendt Aeroelasticitet” under the milestone “Avanceret Rotoraerodynamik – herunder tip- og rodaerodynamik”, (Contract number: ENS-33031-0077) which is carried out by the Aeroelastic Design Group, Wind Energy department at Risø National Laboratory and the Fluid Mechanics Section at the Technical University of Denmark.

In short, the purpose of adding a winglet to a rotor blade design is to decrease the induced drag from the blade by changing the downwash distribution. The art is then to design a winglet, which carries an aerodynamic load such that the vortex from the winglet spreads out the influence of the tip vortex decreasing the downwash and reduces the induced drag. Or in other words; to design a winglet such that the extra form drag, or profile drag, of the winglet is smaller than the decrease in induced drag such that the total drag is decreased. For further reading the theory and physics of winglets on a sailplane is thoroughly described in ref.[i].

In sailplane applications it is most efficient to deflect the tip towards the suction side (pointing upwards) partly due to ground clearance. This leads to a lift on the winglet pointing inwards leading to a wake expansion and thereby emulating the effect of a span increase. In wind turbine applications it is more convenient to point the winglet towards the pressure side (pointing upstream) to avoid tower clearance issues. As a consequence the lift force on the winglet will point outwards. Additionally, since the tip vortex is shed upstream of the rotor plane it will eventually interfere with the vortex sheet from the remaining blades.

The present report describes the aerodynamic investigation of a design change of the tip of a modern wind turbine blade by replacing the original tip with a winglet using computational fluid dynamics. Five different winglets are investigated together with a rectangular shaped tip.

Firstly, a discussion is given of the methodology of generating the blade surface mesh by means of deflecting the outer part of the blade to an angle of approximately 90°. Secondly, the volume mesh generation is described, where special care has to be taken in order for the computational cells to be as orthogonal as possible.

Finally, fully 3D computations have been performed on rotors and compared with the standard rotor without winglets. Results are presented as increase/decrease in mechanical power and thrust as well as spanwise and cross-sectional force and moment distributions and visualisation plots.

1 Winglet design

In the present work it was decided that the outer part of a modern type wind turbine blade should be modified to investigate the effect of adding a winglet. The height of the winglet should be approximately 1.5 % rotor radius and the cant angle (see Figure 1) should be kept at approximately 90º. The sweep angle is set to 0º. Finally, to maximize the effect of the winglet a rectangular tip was assumed.

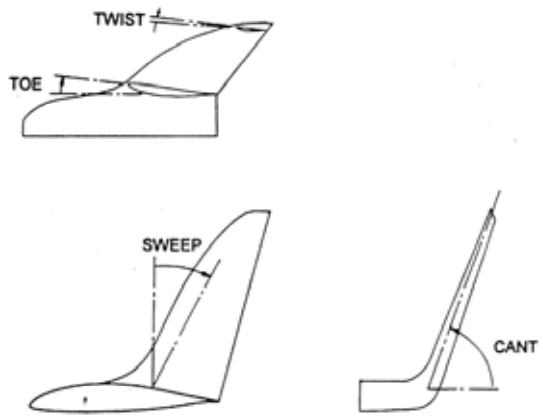

Figure 1: Geometric quantities used to define winglet (from ref.1)

Five different winglet designs have been computed. The first winglet, *winglet1*, has a symmetric NACA 64-018 airfoil section and approximately 0º twist to obtain a C_l of 0.0 as a reference, (green blade in Figure 2). The second winglet, *winglet2*, has a NACA 64-518 airfoil section and a twist of approximately -2º (positive nose down) at the tip to obtain a design C_l of approximately 0.6 (red blade in Figure 2). The third winglet, *winglet3*, is identical to *winglet2* except that it has a tip twist of -5º instead. Based on the results of the first three winglets (see below) two more winglets were designed. In Figure 3 the two final winglets are shown. *winglet4* (white blade in Figure 3) has a tip twist of +3º, while *winglet5* (purple blade in Figure 3) has the same twist as *winglet2*, but the winglet is bended towards the suction side instead. Finally, a rectangular shaped tip, *rectangular*, (not shown in the figures) without winglet, was designed for comparison. For all blades it was decided to keep the rotor radius constant.

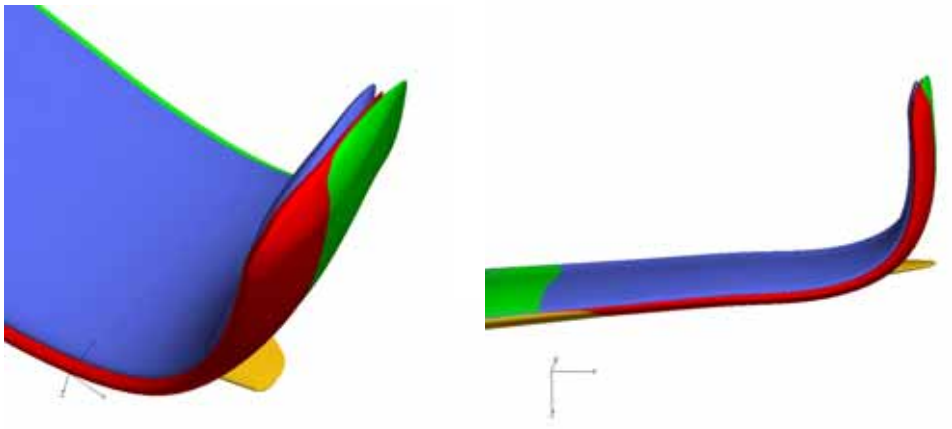

Figure 2: winglet1 (green), winglet2 (red) and winglet3 (blue) compared to the original blade (orange).

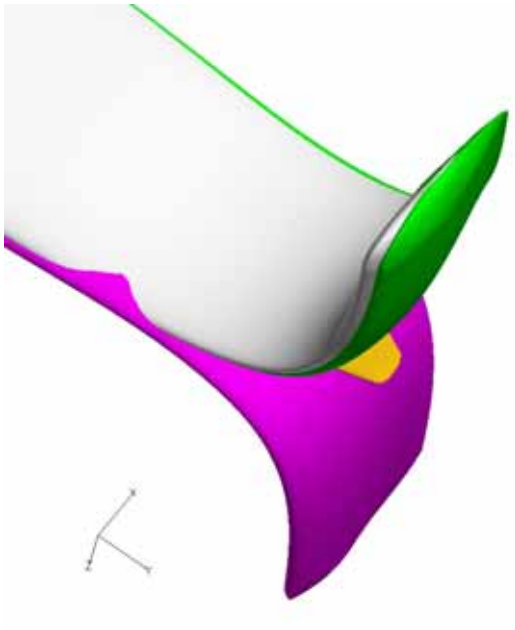

Figure 3: winglet1 (green), winglet4 (white) and winglet5 (purple) compared to the original blade (orange)

The winglets were made be generating a straight blade extending 1.5 % rotor radius further. Following, the 1.5% extension was deflected 90º towards either upstream or downstream direction using a spline representation with seven control points. In this way the final radius was kept the same as the original blade. Looking at the very tip of the winglet it is seen that *winglet2* and *winglet3* are twisted at the tip compared to *winglet1*. Figure 4 shows the chord and twist distribution of the outer 6 % of the blades before deflection of the winglet. (*winglet2*, *winglet3*, *winglet4* and *winglet5* have the same chord distribution as *winglet1* and are therefore not shown.) It is seen that the original blade as well as the rectangular tipped blade extend to r/R = 1, while the blades with winglets extend to r/R =1.015. It is seen that the original blade is designed with a positive twist at the tip (towards lower angles of attack) to minimize the loading. *winglet2* and *winglet3* are designed to increase loading and therefore have a negative twist (towards higher angles of attack). *winglet4* was designed to have the same positive twist at the tip as the original blade. As will be shown below *winglet2* had the best overall performance and therefore *winglet5* was designed with the same twist as *winglet2*, however, *winglet5* is bending towards to suction side.

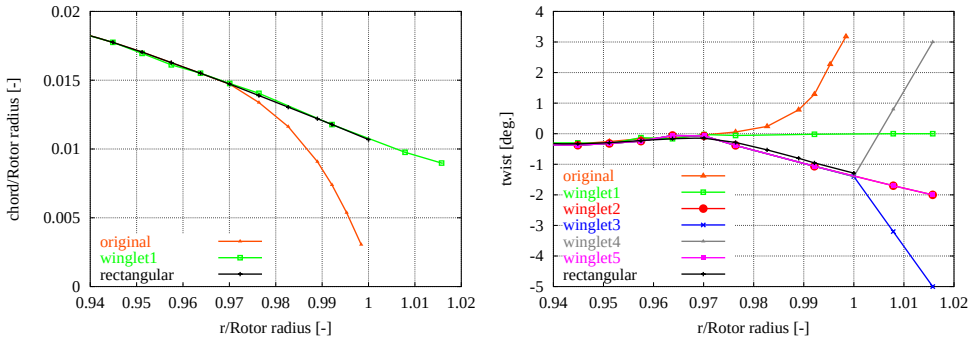

Figure 4: Chord (left) and twist (right) distribution of the outer part of the blades.

Figure 5 shows the rotor equipped with *winglet2* to illustrate the size of the winglet compared to the size of the rotor.

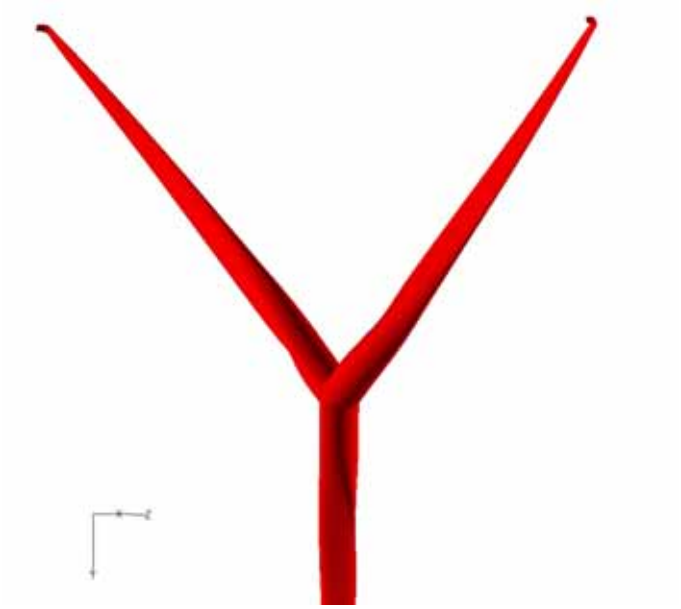

Figure 5: Rotor geometry with winglet2

In Figure 5 it is seen that the computations are made on a rotor only configuration neglecting the nacelle and tower.

2 Generation of computational mesh

The surface mesh is generated using **Gridgen,** a commercial mesh generator developed by **Pointwise, Inc**.

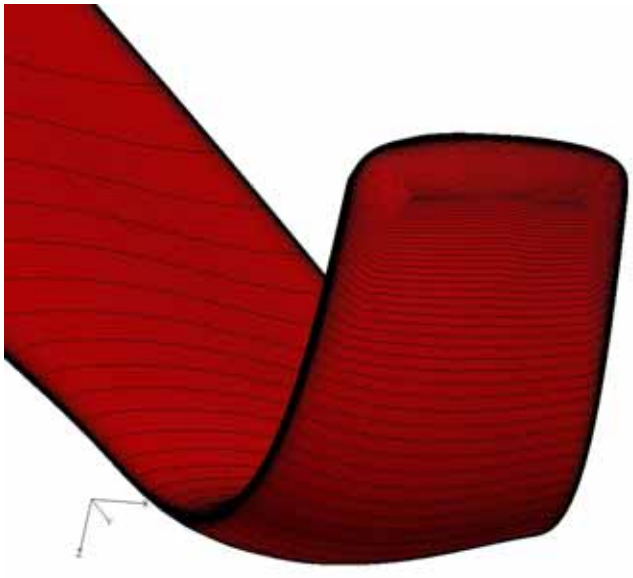

Figure 6: Surface mesh on winglet2.

The volume mesh away from the blade surface is made using the Risø hyperbolic mesh generator HypGrid [ii], which has shown to be more efficient for volume meshing since

restrictions on orthogonality and grid topology are very important. The number of cells on one blade is 256 in the chordwise direction and 128 in the spanwise direction with an additional block of 64x64 on the tip resulting in 36.864 cells on one blade. Away from the surface 128 cells are used with careful control of the stretching. Since the outer boundaries should not affect the solution around the rotor these are placed approximately 10 rotor diameters away. The total number of cells is 432 blocks of 32^3 cells resulting in approximately 14 mio. cells.

3 Results

Computations are made using the Risø/DTU general purpose incompressible Navier-Stokes solver, EllipSys3D [iii], [iv] and [v]. The third order accurate QUICK scheme is used for computing the convective terms and pressure correction are computed using the SIMPLE algorithm. The flow is assumed steady state and turbulence is modeled using the k-ω SST model.

The wind speeds computed are W = 6, 8.5, 10 and 12 m/s and rotational speed and pitch angle at all wind speeds are kept constant. The increase/decrease in mechanical power and thrust compared to the original blade is shown in Table 1 and Table 2.

Table 1: Increase/decrease in mechanical power compared to original blade

Wind speed	*W1 increase*	*W2 increase*	*W3 increase*	*W4 increase*	*W5 increase*	*rect. increase*
6 m/s	1.42 %	-2.23 %	-3.45 %	-1.62 %	1.01 %	-0.61 %
8.5 m/s	0.60 %	1.19 %	0.96 %	0.83 %	1.01 %	0.64 %
10 m/s	0.90 %	1.38 %	1.18 %	0.93 %	1.71 %	1.07 %
12 m/s	1.04 %	1.37 %	1.23 %	0.88 %	1.67 %	1.18 %

Table 2: Increase in thrust compared to original blade

Wind speed	*W1 increase*	*W2 increase*	*W3 increase*	*W4 increase*	*W5 increase*	*rect. increase*
6 m/s	1.44 %	1.44 %	1.44 %	1.81 %	2.89 %	2.17 %
8.5 m/s	0.88 %	1.55 %	1.55 %	1.55 %	1.77 %	1.77 %
10 m/s	1.08 %	1.62 %	1.44 %	1.26 %	1.81 %	1.81 %
12 m/s	1.03 %	1.47 %	1.32 %	1.18 %	1.77 %	1.62 %

To get a visual overview of the individual winglets Table 1 and Table 2 are shown in Figure 7.

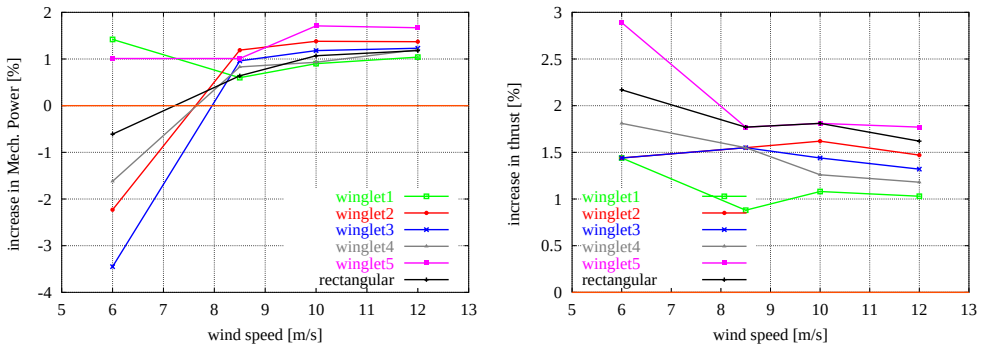

Figure 7: Increase/decrease in mechanical power (left) and thrust (right) compared to the original blade.

There is a slight increase in both power and thrust using winglets (except for *winglet2*, *winglet3, winglet4* and *rectangular* at 6 m/s, see below). For the winglets pointing towards the pressure side *winglet2* gives an overall better power production. *winglet3*, which is twisted to even higher angles of attack, does not produce more power as first expected. This will be investigated in the following. Based on these results the twist of *winglet2* was used for *winglet5*, which instead is pointing towards the suction side. In this way the loading on the winglet is pointing inwards causing a contribution to the wake expansion. Furthermore the tip vortex is moved further downstream of the rotor plane. As expected, *winglet5* results in an even better performance than *winglet2*.

Looking at the spanwise distribution of driving and normal forces, Figure 8, it is seen that the winglets affect the outer approximately 14 % of the blade. Again it is seen that the winglets give rise to a higher driving force at the very tip and *winglet3* has a slightly larger value compared to *winglet2*. But looking further inboard *winglet2* has the highest value leading to overall higher predicted power.

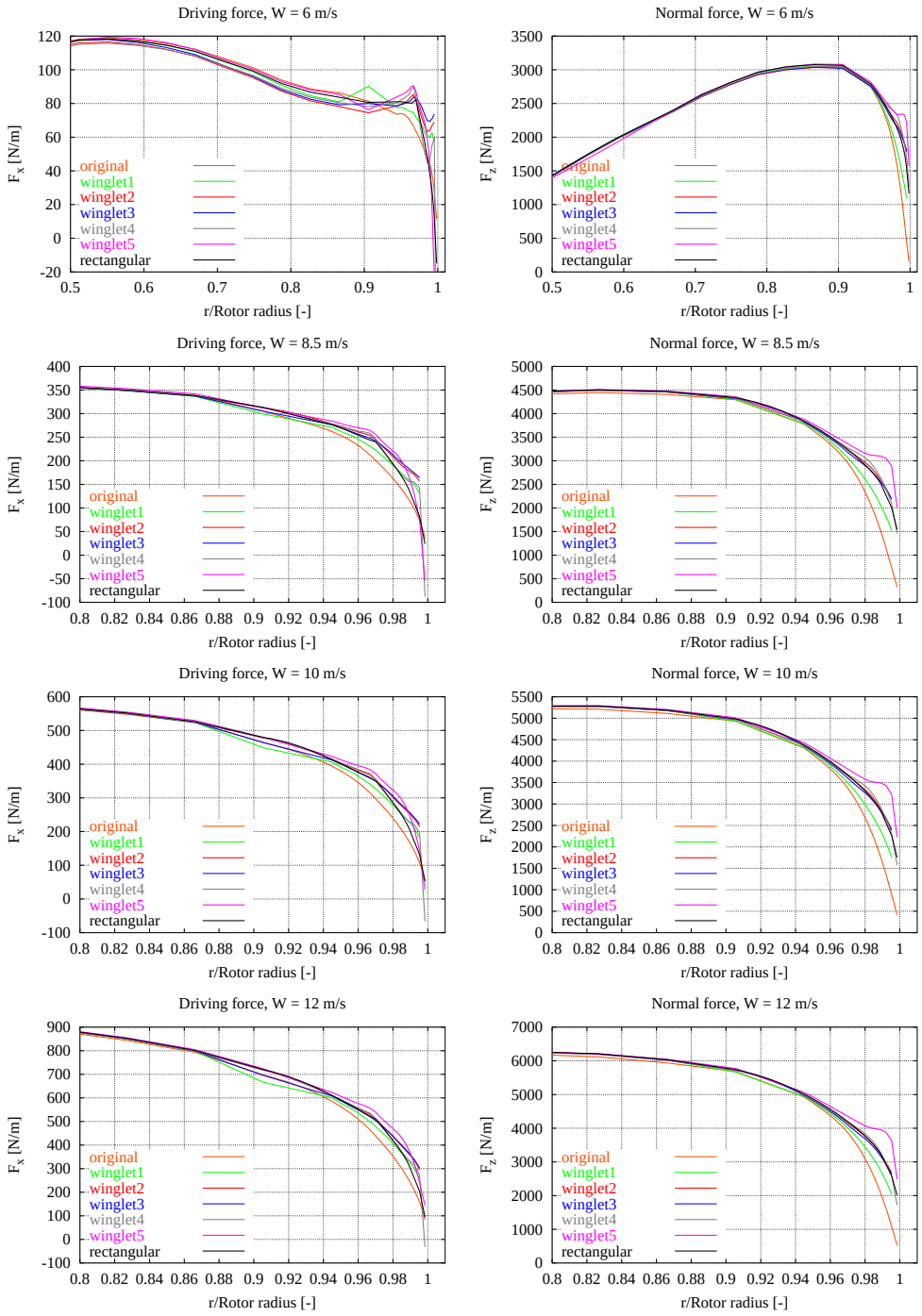

Figure 8: Spanwise distribution of driving force (left) and normal force (right) for W = 6, 8.5, 10 and 12 m/s, respectively.

At 6 m/s, though, the winglets do produce extra driving force near the tip. However, the driving force further inboard is reduced compared to the original blade. *winglet5* shows the largest driving force at the tip and looking at the normal force it is seen that pointing the winglet towards the suction side, the loading is increased compared to the remaining winglets.

There are small local extrema in the driving force at around 90 % radius for *winglet1*. The airfoil geometries at this specific location are identical but looking at the pressure and skin friction distributions for e.g. W = 6m/s, Figure 9, there are small differences in

both pressure and skin friction on the suction side of the leading edge. The small “kinks” in the distributions do probably stem from very small bumps in the surface geometry. It has not been possible to find a plausible physical explanation for this phenomenon.

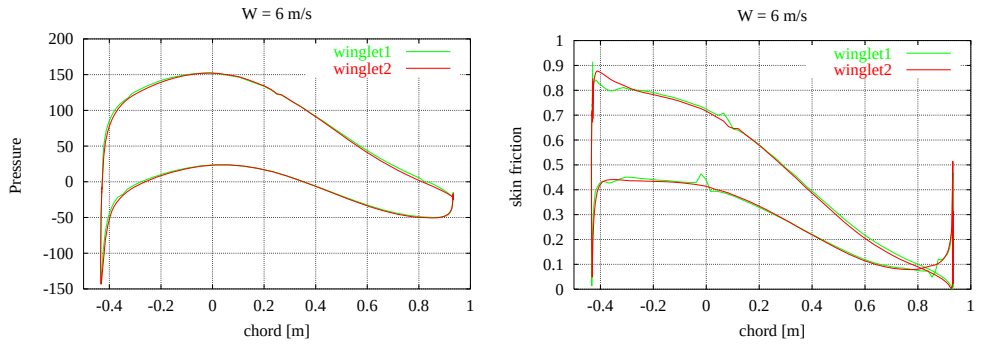

Figure 9: Pressure (left) and skin friction distributions (right) at r/Rotor radius = 90 % for winglet1 and winglet2, W = 6 m/s.

The results for W = 8.5, 10 and 12 m/s all show that *winglet2* and *winglet3* increase driving force compared to both *winglet1*, *rectangular* and *original*.

The general increase in thrust force is partly due to the larger local solidity of the blade tip, but all winglets decrease thrust compared to the rectangular blade except for *winglet5*.

For further analysis of the different winglets it is of importance to determine the cross-sectional forces and moments along the blade. Here this is done by first defining a representative blade axis, which in the present case is given by the midpoint of the blade at x=0 in the r-z plane, blue line in Figure 10.

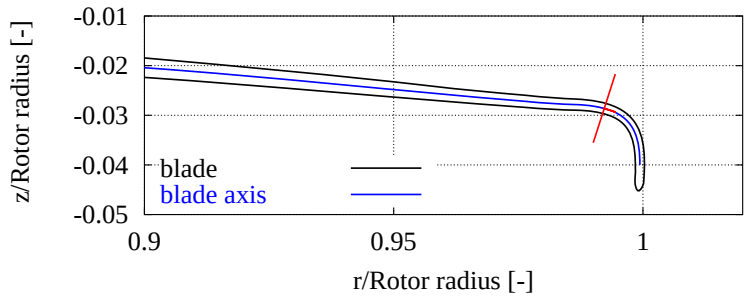

Figure 10: Blade axis definition (blue) as well as a normal plane (red) for winglet2.

At each point along the blade axis the cross-sectional forces and moments are determined in a cut plane normal to the blade axis (e.g. the red line in Figure 10). Figure 11 shows the cross-sectional forces (left) and moments (right) as function of the blade axis length for the outermost 5 %. The five winglets extend approximately 1.5 % further.

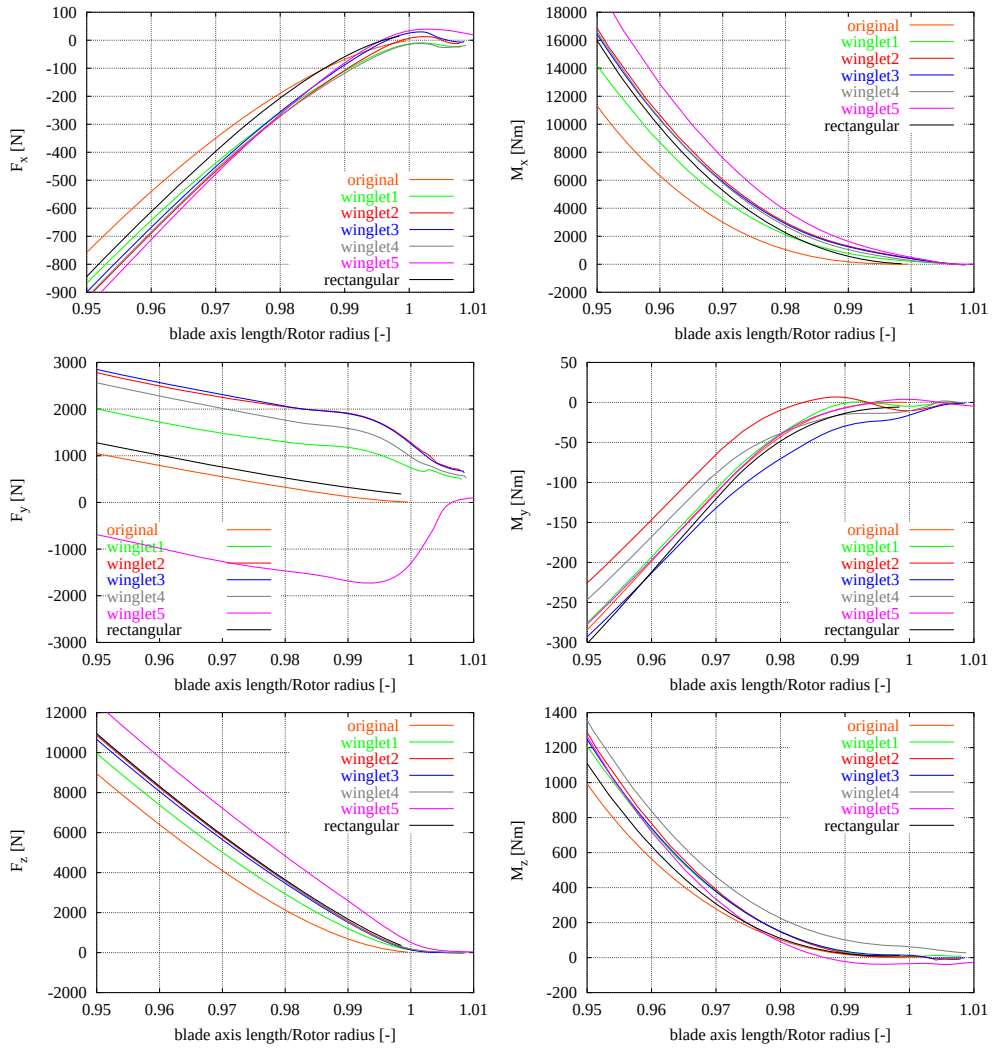

Figure 11: Cross-sectional forces (left) and moments (right) on the outermost 5% of the blade as function of blade axis curve length, W = 10 m/s.

x is pointing in the opposite direction of the driving force, y is pointing in the spanwise direction, while z is pointing in the downstream (thrust) direction. i.e a negative F_x corresponds to a positive cross-sectional driving force. It is seen that the winglets itself (blade axis length/Rotor radius > 1) do not contribute a lot to the driving force, but further inboard *winglet5* and *winglet2* and *winglet4* gives larger forces compared to the original blade and the rectangular tip.

M_x corresponds to the cross-sectional moment around the x-axis which at the root is equal to the root flap moment. Here *winglet5* results in the largest contribution, whereas the original blade has the smallest contribution.

F_y is the cross-sectional force in the spanwise direction positive pointing outwards. The winglets pointing in the upwind direction all have a positive loading while *winglet5*, which is pointing downstream has a loading pointing inwards.

M_y is the local pitching moment and M_z is the local driving moment. Here all five winglets result in larger driving moment in accordance with Table 1. Last, F_z is the local cross-sectional thrust force. Here *winglet5* results in the largest contribution compared to the upwind pointing winglets in accordance with Table 2.

Finally, visualization plots are shown in the following two figures for wind speeds W = 8.5 and 12 m/s, respectively. A pressure contour on the pressure side of the blade surface is shown together with a pressure distribution at a specific location indicated with a black line on the blade. Also shown is a vorticity contour plot 1.0 m behind the blade for visualizing the shed vorticity and the tip vortex. (And not an iso-vorticity as indicated in the figures!)

No large difference is seen comparing the individual pressure distributions at one wind speed. At 12 m/s the suction peek is larger due to the higher incidence angle, as expected. Secondly, looking at the vorticity contour plot it is seen that the tip vortex on *winglet3* is stronger than *winglet1, winglet2* and *winglet4* due to the larger twist leading to a higher loading. Furthermore, the tip vortex is shed from the suction side, i.e. on the outward side of the winglet on the upwind pointing winglets and on the inward side on the downwind pointing winglet.

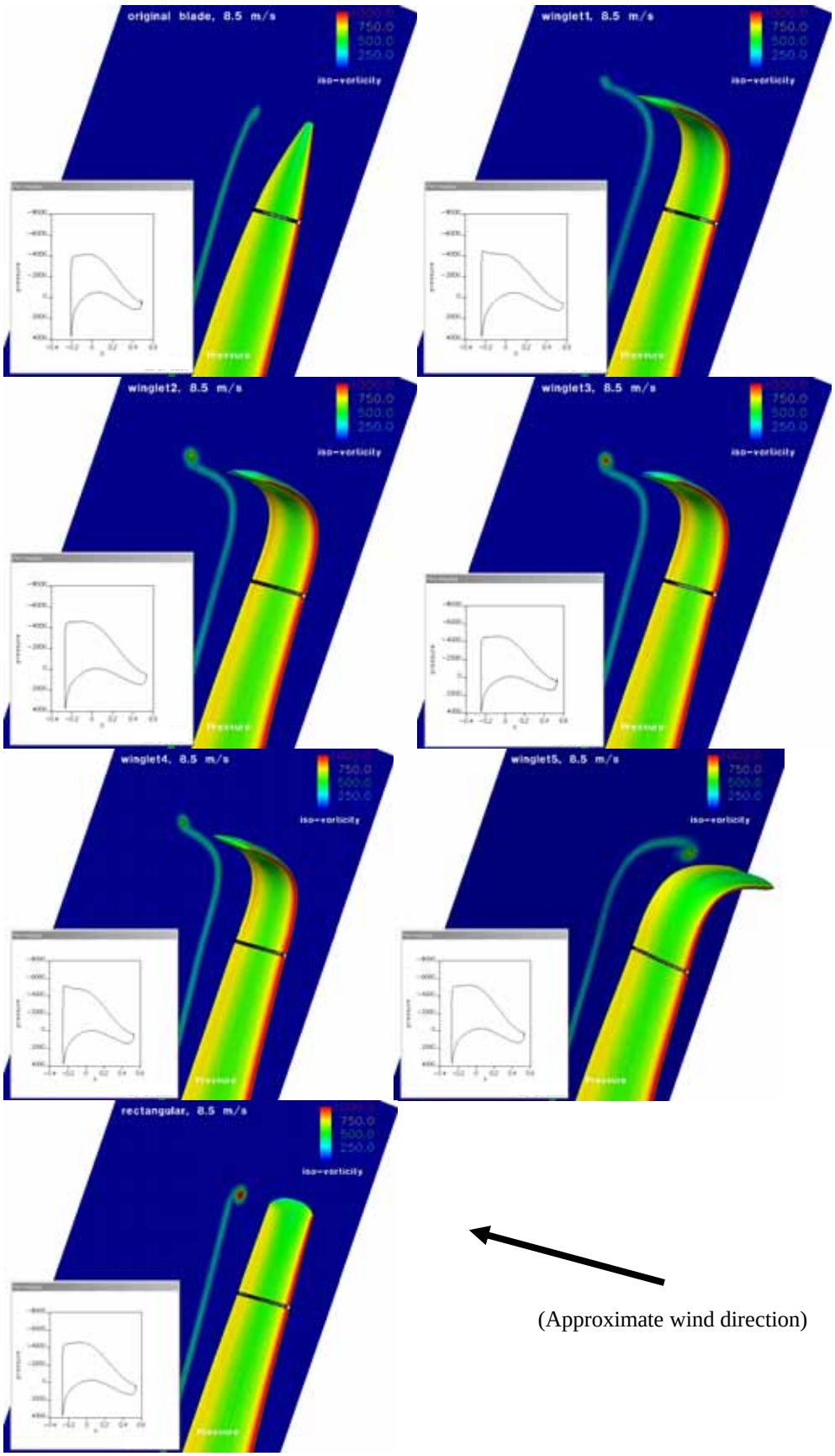

Figure 12: Vorticity contour plot 1.0 m behind the blades and pressure distribution at a specific location, W = 8.5 m/s.

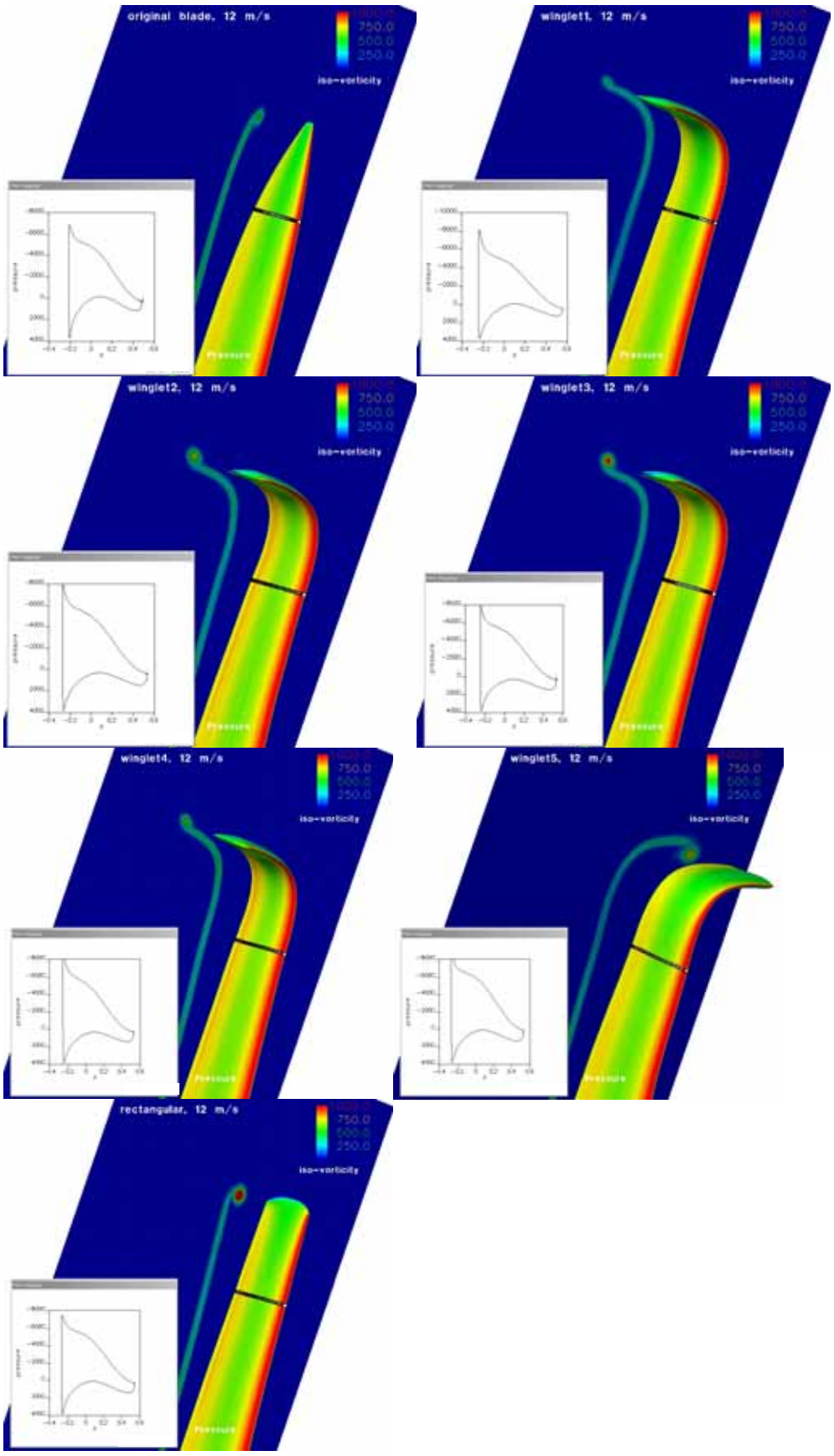

Figure 13: Vorticity contour plot 1.0 m behind the blades and pressure distribution at a specific location, W = 12 m/s.

4 Discussions

There is no doubt that adding a winglet to the existing blade can change the downwash distribution leading to increased produced power, but a load analysis must be made whether the additional thrust can be afforded.

The results on *winglet1*, which were meant to have a C_l of around 0.0, showed that a loading was generated indicating that the effective angle of attack is different from the geometric angle of attack. This is not surprising since total inflow angle is affected by rotation as well as wind speed and local induction.

The results on *winglet2* show an increase in loading due to camber and twist, which also leads to increase in produced power.

winglet3 is twisted even more but does not produce more power compared to *winglet2* even though the flow is not separating.

winglet4 was designed to have to same positive twist at the tip as the original blade and a maximum lift at the bending. This did not result in a more efficient winglet.

Finally, the effect of pointing the winglet towards the suction side (downstream) was investigated. Based on the above mentioned results the twist distribution form *winglet2* was used and resulted in a slightly improved winglet compared to *winglet2*. But still there is the issue of tower clearance.

For comparison a rectangular modification of the original blade tip was designed with the same planform area as the blades with winglets. This modification does produce more power compared to the original blade but not as much as the cambered and twisted winglets. All four upwind pointing winglets do result in lower thrust compared the rectangular blade tip, while the downwind pointing winglet results in comparable or even higher thrust.

Based on the present investigation it is seen that *winglet2* has the best overall power performance of the upwind pointing winglets, but the increase in power of around 1.3% for wind speeds larger than 6 m/s is relatively low and must be compared to the increase in thrust of around 1.6%. But pointing the winglet downstream seems to increase the power production even further. The effect of sweep and cant angles is not accounted for in the present investigation and could improve the performance of the winglets even more.

References

[i] Maughmer M. D., “The Design of Winglets for High-Performance Sailplanes” AIAA Paper 2001-2406

[ii] Sørensen NN “HypGrid2D a 2-D mesh generator”, Risø-R-1035(EN), Risø National Laboratory, Roskilde, Denmark, 1998

[iii] Michelsen JA “Basis3D - a Platform for Development of Multiblock PDE Solvers.”, Technical Report AFM 92-05, Technical University of Denmark, 1992.

[iv] Michelsen JA “Block structured Multigrid solution of 2D and 3D elliptic PDE's.” Technical Report AFM 94-06, Technical University of Denmark, 1994.

[v] Sørensen NN “General Purpose Flow Solver Applied to Flow over Hills.” Risø-R-827-(EN), Risø National Laboratory, Roskilde, Denmark, June 1995.

Mission

To promote an innovative and environmentally sustainable technological development within the areas of energy, industrial technology and bioproduction through research, innovation and advisory services.

Vision

Risø's research **shall extend the boundaries** for the understanding of nature's processes and interactions right down to the molecular nanoscale.

The results obtained shall **set new trends** for the development of sustainable technologies within the fields of energy, industrial technology and biotechnology.

The efforts made **shall benefit** Danish society and lead to the development of new multi-billion industries.